NARR's Atmospheric Water Cycle Components. Part I: 20-Year Mean and Annual Interactions

ALEX C. RUANE

NASA Goddard Institute for Space Studies, and NASA/Oak Ridge Associated Universities Postdoctoral Program, and Sigma Space Partners LLC, New York, New York

(Manuscript received 14 July 2009, in final form 9 March 2010)

ABSTRACT

The North American Regional Reanalysis (NARR) atmospheric water cycle is examined from 1980 to 1999 using a budget approach, with a particular emphasis on annual component interactions and the role of hourly precipitation assimilation. NARR's summertime atmospheric water cycle and diurnal component interactions are examined in Part II of this study. NARR's high-resolution reanalysis and precipitation assimilation allow an improved climatology of mean water cycle components over North America, which is very attractive for applications, climate impact assessments, and as a basis for comparison with other products. A 20-yr climatology of precipitation, evaporation, moisture flux convergence, and the residual error term are produced for comparison to observations, other reanalyses and models, and future climate scenarios. Maps of the normalized covariance of annual precipitation with each of the other water cycle components identify regimes of seasonal interaction that form an additional basis for comparison. The annual cycle of assimilated precipitation is compared to high-resolution precipitation products as an example, and points of interest for continuing studies are identified. Analysis of the mean and transient balances reveals a significant effect from NARR's precipitation assimilation scheme, which is investigated using an estimate of NARR's underlying model precipitation (before assimilation), generated using the precipitation assimilation increment as a proxy. Biases of the precipitation assimilation scheme are then characterized spatially and temporally to inform the interpretation of NARR applications and comparisons. These model precipitation estimates reveal a more tightly closed atmospheric water cycle with predominantly excessive precipitation, resulting in too vigorous evaporation and moisture flux convergences. The sign and magnitude of evaporation and moisture flux convergence biases are found to be related to the precipitation assimilation correction and are important to consider in applications of NARR output.

1. Introduction

Regional hydrometeorological and hydroclimatological applications require long-term, consistent datasets for analysis, particularly those with the capability to drive further downscaling of river basins or particular impact sectors. Retrospective analyses (reanalyses) are often used for these purposes, but they have well-known biases relating to precipitation parameterizations in many parts of the world (particularly at seasonal and diurnal time scales; e.g., Ruane and Roads 2007a; Trenberth et al. 2003). In an investigation of a global reanalysis product, Ruane and Roads (2008, hereafter RR2008) replaced the parameterized precipitation forecast with rainfall from a satellite-based high-resolution precipitation product, finding that water cycle component interactions more completely described important hydrologic features, such as the nocturnal maximum in summertime rainfall over the U.S. upper Midwest, when precipitation had appropriate variation. This crude swap is not internally consistent, however, and should be improved upon by a true precipitation assimilation system with dynamical interaction between assimilated precipitation and other components of the water and energy cycles.

The North American Regional Reanalysis (NARR; Mesinger et al. 2006) provides a unique opportunity to examine the water cycle at high spatial and temporal scales, and it differs most strikingly from the global reanalyses in its incorporation of hourly precipitation assimilation. The impressive matches between NARR's assimilated precipitation fields and observations suggest that the entire water cycle may be dramatically

Corresponding author address: Alex Ruane, NASA Goddard Institute for Space Studies, 2880 Broadway, New York, NY 10025. E-mail: aruane@giss.nasa.gov

DOI: 10.1175/2010JHM1193.1

© 2010 American Meteorological Society

improved, making NARR a prime candidate for hydrometeorological and hydroclimatological applications. Precipitation assimilation introduces budget errors that are not trivial; however, the NARR developers have retained extensive water cycle variables that aid in the interpretation of NARR applications by allowing for a careful accounting of associated biases.

This study has three main parts. First, NARR's mean water cycle is examined from 1980 to 1999, providing a 20-yr climatology that may serve as a basis for comparison with observations, other models, reanalysis products, climate models, and future scenarios [e.g., from the North American Regional Climate Change Assessment Program (NARCCAP); Mearns et al. 2009]. Second, annual water cycle component interactions with precipitation are examined to identify key precipitating regimes that may potentially be sensitive to climate changes. Lastly, a portion of the water cycle residual error terms are attributed to precipitation assimilation by estimating the water cycle before and after precipitation assimilation occurs. Ruane (2010; hereafter Part II) examines NARR's mean summertime atmospheric water cycle (when convective systems predominate), diurnal component interactions, and the corresponding biases attributable to precipitation assimilation.

This study builds on previous examinations of the atmospheric water cycle in global reanalysis systems (e.g., Trenberth and Guillemot 1998; Roads et al. 2002), their component interactions (RR2008), and residual error terms including an analysis increment (Schubert and Chang 1996; RR2008). In addition to the novel precipitation assimilation, NARR's regional focus and higher resolution allow for an improved representation of moisture flux convergence and boundary layer processes. The examination of isolated seasonal variability is motivated in part by a previous study (Ruane and Roads 2007a) that demonstrated that mean water cycle statistics can miss the tendency of some parameterizations to shift variance to longer time scales to reproduce particular modes of variability, such as the El Niño–Southern Oscillation.

NARR's domain is one of the best observed regions in the world, featuring complex interactions among water cycle components that make it an excellent test bed for hydrometeorological analyses (Rasmusson 1967, 1968; Berbery et al. 1996; Betts et al. 1999; Nigam and Ruiz-Barradas 2006). Major hydroclimate studies of the region include the Global Energy and Water Cycle Experiment (GEWEX) Americas Prediction Project (GAPP) over the Mississippi River basin (Roads et al. 2003), the Mackenzie GEWEX Study (MAGS; Szeto et al. 2008), and the North American Monsoon Experiment (Higgins et al. 2006).

NARR is briefly described in the next section. Its mean atmospheric water balance, precipitation assimilation sources and technique, and the normalized covariance methods employed in this study are presented in section 3. Section 4 describes the 20-yr mean balance of water cycle components, while section 5 analyzes the interactions of precipitation with other water cycle components on the annual scale. A brief summary and potential future works are described in section 6, along with a discussion of the implications of the results.

2. NARR

The National Centers for Environmental Prediction's (NCEP) NARR was designed as a ''long-term, dynamically consistent, high-resolution, high-frequency, atmospheric and land surface hydrology dataset for the North American domain'' (Mesinger et al. 2006). Boundary conditions and many of the assimilation parameters come from the NCEP/Department of Energy Global Reanalysis 2 (R2; Kanamitsu et al. 2002), but the contrast between the two reanalysis systems is striking. The R2 has global ~1.9° horizontal resolution with 28 σ layers and a two-layer land surface model; it assimilates observations every 6 h and utilizes the simplified Arakawa–Schubert convective parameterization with a 5-day pentad soil moisture adjustment. NARR features 32-km resolution with 45η levels and the four-layer Noah land surface model (Ek et al. 2003), assimilates observations every 3 h, and utilizes the Betts–Miller–Janjić convection scheme (Janjić 1994), which is then adjusted according to the hourly precipitation assimilation (described in the next section).

NARR covers the 25-yr period from 1979 to 2003 (available online at http://www.emc.ncep.noaa.gov/mmb/rreanl) and is being continued with a slightly modified version to the present. The 1980–99 portion analyzed in this study was chosen as a representative climatology to facilitate comparisons to twentieth-century simulations by global climate models analyzed in the Fourth Assessment Report of the Intergovernmental Panel on Climate Change (Solomon et al. 2007), which often end in 1999.

NARR's ability to constrain the land surface with observed precipitation has a large benefit with regard to evaporation relative to other reanalyses (Mesinger et al. 2006). Thus, most of the studies analyzing the water cycle in NARR have focused on surface water processes or land–atmosphere interaction (e.g., Luo et al. 2007; Karnauskas et al. 2008; Vivoni et al. 2008; Dominguez and Kumar 2008; Yilmaz et al. 2008). Studies of NARR's atmospheric water cycle are less common (e.g., Nigam and Ruiz-Barradas 2006; Ruiz-Barradas and Nigam 2006; Nunes and Roads 2007). NARR is currently an excellent

basis for comparison of independent global and regional simulations (e.g., Ruane and Roads 2007b; Kanamaru and Kanamitsu 2007), but it is important to remember that NARR's reanalysis system includes model and assimilation error and thus is not identical to observations. Part II of this study shows that this is especially true for the diurnal cycle.

3. NARR's atmospheric water balance

a. Water cycle components

Natural variations in precipitable water tendency T occur corresponding to additions of moisture through the sides of the column via moisture (vapor and condensate) flux convergence C, additions of moisture from the surface via evaporation E, and losses of moisture as precipitation P falls out of the column. These terms are expressed in the following theoretical water cycle balance:

$$T = C + E - P. \tag{1}$$

Artificial influences, however, also contribute to a precipitable water tendency between analysis times in NARR. As will be discussed in the next subsection, NARR adjusts the water column to account for discrepancies between the precipitation simulated by NARR's underlying Eta model (based on Black 1994) and the observed precipitation. Additionally, a model analysis increment in precipitable water, common to all reanalyses, results from the discrepancy between the model's atmospheric state entering an analysis interval and that which follows after new observations are assimilated, among other things capturing spin-up biases, errors introduced by insufficient resolution, and the redefinition of model layers (Schubert and Chang 1996). NARR also employs a horizontal advection scheme that adjusts moisture distributions to match larger-scale patterns (Janjić 1997). A better representation of NARR's water cycle may therefore be obtained by including these terms in an aggregate residual error term (r) that is calculated to precisely balance the following budget:

$$T = C + E - P + r. \tag{2}$$

b. Sources of assimilated precipitation

NARR assimilates precipitation from a patchwork of sources across its domain (Shafran et al. 2004). Gauge observations are most extensive over the contiguous United States, where NARR uses on average 17 500 daily reports from the National Climatic Data Center's daily cooperative stations, River Forecast Center stations, and daily accumulations of the hourly precipitation dataset (see Higgins et al. 2000). The latter dataset utilizes the Precipitation-elevation Regressions on Independent Slopes Model (PRISM; Daly et al. 1994) to augment precipitation values over mountain slopes. Over Canada and Mexico, daily precipitation values come from a 1° gauge-based dataset, with U.S. borders blended to minimize spatial discontinuities with Canadian and Mexican datasets. Oceanic precipitation is drawn from the Climate Prediction Center Merged Analysis of Precipitation (CMAP; Xie and Arkin 1997), a 2.5° dataset combining satellite and gauge data in pentads. Lack of satellite measurements makes CMAP precipitation unreliable at high latitudes, so no precipitation is assimilated north of 42.5°N over the oceans, Alaska, and most of Greenland. Precipitation in these areas is the direct output of NARR's underlying Eta model, and a 15° latitudinal band centered on 42.5°N blends the assimilated precipitation region to the south with the model precipitation to the north. Model precipitation also replaces CMAP precipitation in areas showing more than 100 mm day^{-1} of precipitation and over tropical storms. Mesinger et al. (2006) recommend applications over land, particularly in areas of high-density precipitation observations. Precipitation over the Caribbean islands and Hawaii were not assimilated, often leading to spurious results.

Further processing of these datasets casts the daily and pentad precipitation totals to hourly values that may be used in NARR's precipitation assimilation scheme. These processes are irrelevant on the annual frequencies analyzed here, but they are detailed in the examination of NARR's diurnal cycle in Part II of this study.

c. Precipitation assimilation

As will be shown in the next section, the size of the residual error term (both in its mean and its annual variation) may be disconcerting for some NARR users. A portion of these errors may be attributed to the precipitation assimilation process, however, so this subsection provides a brief overview of NARR's approach and derives an estimate of the underlying model's precipitation (before precipitation observations are assimilated) to characterize associated biases for the interpretation of NARR applications.

Precipitation assimilation in NARR is undertaken with a strategy of adjusting the hourly latent heating to account for the discrepancy between modeled and observed precipitation while maintaining realistic moisture profiles (Mesinger et al. 2006). This basic approach was first proposed by Krishnamurti et al. (1984), and similar approaches have been put to wide use (e.g., Monobianco

et al. 1994; Yap 1995; Nunes and Roads 2005). NARR's assimilation method is detailed by Lin et al. (1999), and its application to the NCEP Meso Eta Analysis and Forecast System is described in Rogers et al. (2001). A short description of the relevant procedures (Y. Lin 2008, personal communication) is provided here to enable interpretation of the NARR results presented later.

Precipitation assimilation is conducted on an hourly basis, which is more frequent than NARR's general 3-hourly data assimilation. In the case of a discrepancy between the amount of precipitation produced by NARR's underlying model (P_{mod}) and the observed precipitation P_{obs}, the precipitation assimilation scheme attempts to maintain a reasonable relative humidity while modifying the column energy profile and altering the moisture content to adjust the convective stability in the convective parameterization that produced biased results. For example, if the model produces excessive precipitation, then the latent heating in the column is reduced to mimic a slowed precipitation rate and column moisture is reduced to eliminate the moisture excess. NARR's precipitation assimilation achieves a close approximation of observed precipitation, constraining the amount of moisture that reaches the soil column for an improved representation of evaporation that feeds back through the entire water cycle.

The result of these precipitation assimilation adjustments is a net gain or loss in moisture. Were the precipitation assimilation scheme perfectly balanced in terms of the water cycle, moisture would be added back to the atmospheric column at a rate equivalent to an excess in modeled precipitation (compared to observations) or would be removed from the atmospheric column at a rate equivalent to a deficit in modeled precipitation. In practice, however, this would require an increase in moisture where the model produced too much precipitation compared to observations and a reduction of moisture in regions where the model produced less precipitation than was observed—an exacerbation of the model's deficiencies. Rather than exacerbate the model's deficiencies for the sake of a closed budget, NARR's precipitation assimilation scheme uses moisture increments to reduce inappropriate moisture tendencies in the model's atmospheric column versus observations. NARR output accounts for the precipitation assimilation adjustments of water vapor (VI; applied to adjust relative humidity) and water condensate (CI; applied to impose or reduce cloud layers), together forming the assimilation increment I applied to the atmospheric column,

$$I = \mathrm{VI} + \mathrm{CI}. \tag{3}$$

Additionally, the discrepancy D between P_{mod} and the assimilated P that is reported in NARR output is also a moisture imbalance:

$$D = P - P_{\mathrm{mod}}. \tag{4}$$

While I may be obtained in the NARR output, D is not available. The P_{mod} is also not reported, but its estimation allows us to compare NARR's water budget with the water balance of its underlying model before assimilation occurs, revealing the value added by the precipitation assimilation scheme. Without a means to directly calculate P_{mod}, it is helpful to define the following model precipitation estimate M:

$$M \equiv P - I = P_{\mathrm{mod}} + D - I. \tag{5}$$

The difference between M and P_{mod} is thus related to the difference between I and the discrepancy between modeled and assimilated precipitation D. The I and D almost always have the same sign (Y. Lin 2008, personal communication), and larger D results in a larger I, although their relationship is not linearly proportional because of nonlinearities in the Clausius–Clapeyron equation and the range of relative humidities at which precipitation may occur. The estimation error between M and P_{mod} is therefore smaller in magnitude than both D and I, but its sign is not known. Use of M here is not meant to precisely quantify precipitation-assimilation-related biases, but rather to guide interpretations of NARR applications in light of these biases.

To investigate NARR's water cycle, we will thus consider two water budgets. The first was introduced in Eq. (2), representing the water cycle as reported in NARR's standard output. The second is an approximation of the water budget of NARR's underlying model, generated by replacing P in Eq. (2) with $M + I$ [according to Eq. (5)] and rearranging as follows:

$$T + I = E + C - M + r. \tag{6}$$

The right-hand-side (rhs) of this equation has the same representative terms as the rhs of Eq. (2). However, M differs from the assimilated P that is reported in NARR's output. Here, r is the same in both equations, containing elements such as the model reinitialization increment, moisture lost due to precipitation assimilation, and errors due to the horizontal advection routine.

Although Eq. (7b) is an estimate of the model's water cycle before precipitation assimilation, the underlying model is disrupted on an hourly basis by precipitation assimilation adjustments that lead to imbalances in the estimated underlying water cycle. The term I is directly proportional to the magnitude of these imbalances, so pairing it with the reported precipitable water tendency

on the left-hand-side of Eq. (7b) provides a better gauge of the underlying model changes in NARR's precipitable water.

d. Transient analysis using normalized covariance

The use of normalized covariances as a means to explore the water cycle was introduced in RR2008 and will only be briefly reviewed here.

Each term in NARR's assimilated water budget [Eq. (2)] and model water budget [Eq. (6)] may also be considered as a sum of its mean (denoted with an overbar) and transient (denoted by a prime) components

$$(\overline{T} + T') = (\overline{E} + E') + (\overline{C} + C') - (\overline{P} + P') + (\overline{r} + r') \quad \text{and} \tag{7a}$$

$$(\overline{T} + T') + (\overline{I} + I') = (\overline{E} + E') + (\overline{C} + C') - (\overline{M} + M') + (\overline{r} + r'). \tag{7b}$$

Each balance therefore holds over its long-term mean

$$\overline{T} = \overline{E} + \overline{C} - \overline{P} + \overline{r} \quad \text{and} \tag{8a}$$

$$\overline{T} + \overline{I} = \overline{E} + \overline{C} - \overline{M} + \overline{r} \tag{8b}$$

and among the transients at any orthogonal frequency

$$T' = E' + C' - P' + r' \quad \text{and} \tag{9a}$$

$$T' + I' = E' + C' - M' + r'. \tag{9b}$$

To isolate the transient components of the water cycle at annual frequencies, daily averages of each water cycle component were constructed from NARR's 3-hourly output. Each year was then passed through a broadband Fourier filter that captured the variance contained in the first four variance bands, representing periods between approximately 90 and 365 days. The inclusion of harmonics that repeat 2, 3, and 4 times per year captures the low-frequency character of the annual cycle at most locations far more accurately than a perfect 365-day harmonic does, and thus we refer to the filtered series as the annual signal. After solving for P', the covariance of P' with each other term in Eq. (9a) is then normalized by the variance of P', and likewise for M' in Eq. (9b). The result is the following relationship, which describes 100% of the annual variation of P' or M' through their normalized covariance with the other water budget terms:

$$\frac{\mathrm{cov}(P', P')}{\mathrm{var}(P')} \times 100\% = \frac{\mathrm{cov}(E', P') + \mathrm{cov}(C', P') + \mathrm{cov}(-T', P') + \mathrm{cov}(r', P')}{\mathrm{var}(P')} \times 100\% = 100\% \quad \text{and} \tag{10a}$$

$$\frac{\mathrm{cov}(M', M')}{\mathrm{var}(M')} \times 100\% = \frac{\mathrm{cov}(E', M') + \mathrm{cov}(C', M') + \mathrm{cov}(-[T' + I'], M') + \mathrm{cov}(r', M')}{\mathrm{var}(M')} \times 100\% = 100\%. \tag{10b}$$

Terms in the central portion of Eqs. (10a) and (10b) were called "normalized covariances" in RR2008, and are the basis of annual water budget analysis in this study. These normalized covariances, computed for each year and then averaged over the 1980–99 period, indicate the percentage contribution that each water cycle component makes toward precipitation's variance at the annual scale. Any annual variation leading to an increase in precipitation must be balanced by a corresponding increase in evaporation, increase in moisture flux convergence, decrease in the precipitable water column, or increase in the error term of the water budget. Often, the moisture lost to precipitation comes from a combination of these sources. These normalized covariances complement the classic precipitation recycling metric, which does not isolate specific modes of variability in the water cycle (Dirmeyer and Brubaker 2007).

For example, the first term in the center of Eq. (10a) is the normalized covariance of precipitation with evaporation. If $\mathrm{cov}(E', P')/\mathrm{var}(P') = 100\%$, the variation of evaporation matches the variation of precipitation on the annual scale. If this term is 0%, there is no annual covariant relationship between evaporation and precipitation. If this term is >100%, evaporation varies mostly in phase with precipitation but with a greater annual amplitude. If this term is <0%, evaporation is out of phase with precipitation at this time scale. If this term is between 0% and 100%, evaporation's phase or amplitude deviates from precipitation's annual signal and evaporation only makes a partial contribution to the moisture lost through precipitation.

When interpreting these normalized covariance terms for annual component interactions, it is important to recognize several key caveats. First, it is difficult to separate the relative contributions of phase and amplitude in covariance (and thus normalized covariance). Second, dividing by the precipitation's variance can lead to very large normalized covariances in regions with low precipitation variance (typically dry areas), so values in areas with high mean rainfall are more robust. Lastly,

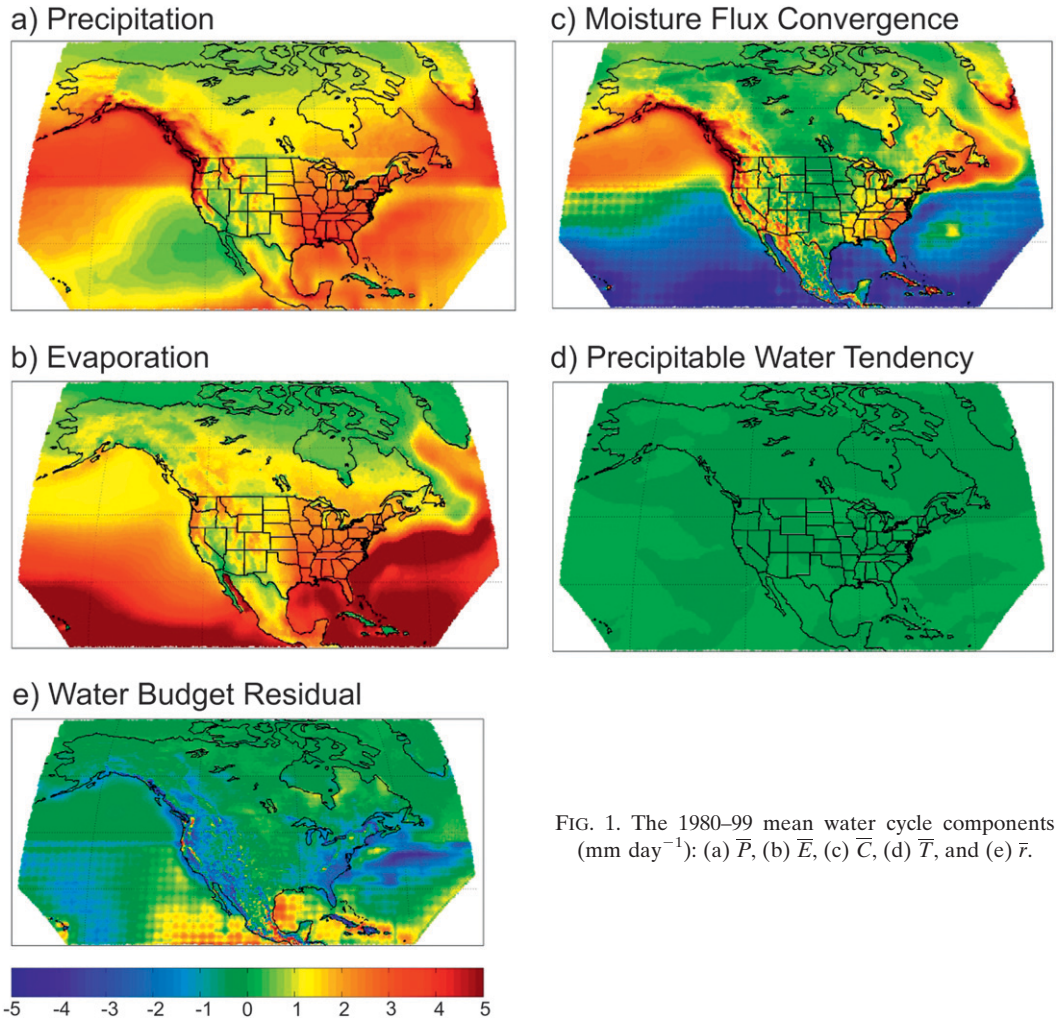

FIG. 1. The 1980–99 mean water cycle components (mm day^{-1}): (a) $\overline{P}$, (b) $\overline{E}$, (c) $\overline{C}$, (d) $\overline{T}$, and (e) $\overline{r}$.

these normalized covariances represent annual variations on top of mean conditions, and they underscore that the water cycle balance at a particular mode of variability can occasionally counteract mean characteristics. In general, normalized covariances help identify interesting water cycle behaviors, but additional analysis is required for precise causation.

4. 20-yr mean balance

Figure 1 presents maps of the NARR water cycle components' 20-yr means, as expressed in Eq. (8a). These maps reveal the balance averaged across all frequencies of variation. A subset of the NARR domain is shown to focus detail on the North American continent.

The general climatology of North American precipitation is well known, and NARR succeeds in producing a close match with added resolution and detail (Mesinger et al. 2006). Precipitation over land is heaviest over the southeastern United States and the coastal ranges of the Pacific Northwest. Local minima along international borders are signatures of NARR's assimilation of multiple sources of observed precipitation, as the blending region results in a reduction of precipitation compared to either side (Mo et al. 2005). Precipitation over the oceans also shows clear artifacts of the precipitation assimilation scheme. A stark boundary at 42.5°N separates areas forced by CMAP precipitation (to the south) from areas with no precipitation assimilation (to the north). High mean precipitation in areas without precipitation assimilation suggests that the underlying model has a wet bias over the oceans.

Mean evaporation in NARR closely resembles mean precipitation patterns over the eastern United States, Mexico, and the interior of Canada, suggesting a strong balance in these regions on this long time scale. The tight match between evaporation and the assimilated

precipitation fields underscores the appeal of using a reanalysis with precipitation assimilation for hydrologic applications. Oceanic evaporation exceeds precipitation amounts and increases rapidly with sea surface temperatures, leading to strong moisture flux divergence over warm waters.

NARR's moisture flux divergence from warm marine air masses results in a massive redistribution of moisture to cool marine air masses at high latitudes and to the continent where it eventually becomes surface runoff. The dynamics of this key moisture transport, captured by NARR at high spatial and temporal resolution, have significant implications for the climate of North America. A strong balance between precipitation and moisture flux convergence is apparent over the west coasts of the United States and Canada, where marine air masses drop large amounts of water as they are forced over the coastal mountain ranges. Orographic enhancement of precipitation also appears as moisture flux convergence along the windward flanks of interior mountain ranges. NARR produces substantial moisture flux convergence over the North American monsoon regions of northern Mexico and the southwestern United States, which may be biased toward too much convergence (Becker and Berbery 2008). Despite the presence of a summertime low-level jet (Higgins et al. 1997) that transports a large flux of moisture into the Midwest of the United States from the Gulf of Mexico, this moisture results in only a small net convergence when averaged over this long period (Anderson et al. 2009). The bull's-eye patterns of convergence over the oceans have similar resolution and coverage to the CMAP product, and are likely an artifact of the precipitation assimilation routine (Bukovsky and Karoly 2007).

As expected, NARR's mean precipitable water tendency is negligible over the 20-yr period. Compared to the flux terms that accumulate over the decades, precipitable water does not have any significant net tendency.

As precipitation is constrained to observed values, water cycle budget residuals infer biases in the other water cycle components that inform analyses and applications of NARR output. According to Eq. (8a), those locations showing positive moisture budget residuals in NARR indicate that evaporation and/or moisture flux convergence is too low or that precipitation is too high. Negative residuals indicate that either precipitation is too low or evaporation and/or moisture flux convergence is too high. Although smaller than the precipitation, evaporation, and moisture flux terms in most locations, NARR's water budget residual is substantial. As discussed in the previous section, this error term contains a 3-hourly analysis increment and errors introduced by the discontinuous hourly precipitation assimilation scheme, among other possible error sources. Negative residuals over the western mountain ranges are likely due to the analysis increment, as inconsistencies between model and true topography often lead the model water cycle astray. Large residuals in other locations motivate a better understanding of the precipitation assimilation scheme, which is a leading candidate to explain these imbalances. The 42.5°N demarcation and bull's-eye signature of CMAP assimilation is clear in the residuals over the oceans, but precipitation assimilation's overall contribution to water budget imbalances over land is best understood by looking directly at the precipitation assimilation increment terms.

Figure 2 displays the 20-yr mean assimilated precipitation as well as its model precipitation and assimilation increment components, as expressed in Eqs. (3) and (5). The water vapor and water condensate assimilation increments show that NARR's precipitation assimilation has its largest effect over the Atlantic Ocean, most strikingly on the northern edge of the Gulf Stream. Large amounts of moisture are also incorporated by the precipitation assimilation scheme over the central Pacific, the intertropical convergence zone (ITCZ), and the eastern portion of the continent (especially Florida). The assimilation increments are overwhelmingly negative, indicating that precipitation assimilation most often reduces overly active model precipitation, although the Maritime Provinces and some mountainous portions of the western United States display small positive increments. Although the water condensate and water vapor increments are very similar, water condensate increments are smaller over the Rockies, central Mexico, and much of Canada. Positive increments are almost exclusively due to water vapor adjustments, indicating more need for increasing relative humidities than for imposing new rain clouds. The water vapor increment dominates adjustments (both positive and negative) over the western mountain ranges, where the analysis increment is forced to rectify discrepancies in the complex terrain.

Estimates of the model precipitation prior to precipitation assimilation (Fig. 2b), calculated following Eq. (5), reveal wet biases across much of the domain in NARR's underlying Eta model compared to the assimilated precipitation (Fig. 2a). These biases are proportional to mean model precipitation, but they are also related to the main component interactions that lead to precipitation. The negative residuals associated with precipitation assimilation reflect that the reduction of model precipitation to observed values is not balanced by corresponding reductions to the local evaporation or moisture flux convergence terms, which are not directly affected by the precipitation assimilation scheme. Close correspondence between precipitation assimilation regions

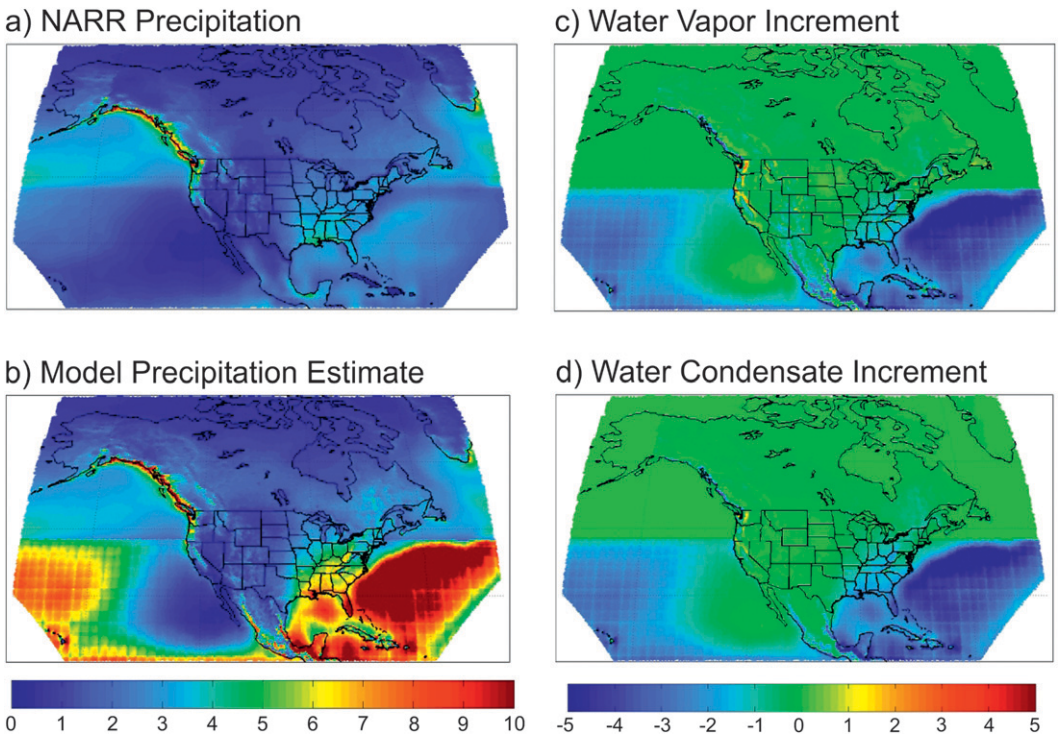

FIG. 2. The 1980–99 mean precipitation assimilation components (mm day^{-1}): (a) NARR $\overline{P}$, (b) $\overline{M}$, (c) $\overline{\mathrm{VI}}$, and (d) $\overline{\mathrm{CI}}$. Note that the color bars for the precipitation terms in (a) and (b) are different from the color bars for the assimilation terms in (c) and (d).

and regions of high evaporation suggests that this imbalance comes primarily from the evaporation field, indicating a high evaporation bias in NARR that must be factored into hydrological applications. This bias in evaporation has been suggested (Nigam and Ruiz-Barradas 2006; Kanamaru and Kanamitsu 2007; West et al. 2007), but the mean maps shown here and the annual variations presented in the next section elucidate these further. Similar patterns are also apparent (to a slightly lesser extent) in regions with high moisture flux convergence. Additionally, a comparison between Figs. 2c and 2d and Fig. 1e allows NARR users to roughly gauge the influence of precipitation assimilation increments in the overall residual error term at any given location.

5. Annual component interactions

The precipitation and atmospheric state variables that constrain NARR to observations are assimilated on a much shorter time scale than the seasonal patterns that make up annual variation. Thus, NARR precipitation's annual variation may be used as a reliable basis for comparison to other precipitation sets. The evaporation and moisture flux convergence fields, however, rely heavily on internal model thermodynamics and dynamics, respectively. The normalized covariance of each water cycle component with annual precipitation is examined in this section to isolate climatological exchanges that may be compared among observational datasets, reanalyses, and climate models under various scenarios. The effects of NARR's precipitation assimilation scheme are also investigated to interpret the implications of NARR's water budget imbalances associated with seasonal variation.

To understand the nature of the annual variance that forms the basis of this examination, Fig. 3 shows the simple annual harmonic of precipitation from NARR for comparison to the R2 and two high-resolution precipitation products (HRPPs). These HRPPs (briefly described in Ruane and Roads 2007a), the Climate Prediction Center morphing method (CMORPH; Joyce et al. 2004), and Precipitation Estimation from Remotely Sensed Information using Artificial Neural Networks (PERSIANN; Hsu et al. 1997), use a combination of polar-orbiting instruments and ground-based rainfall measurements to train geostationary satellite information to pick up rainfall rates with nearly global coverage equatorward of $\pm 60°$ latitude. NARR provides a comparison to gauge these products' performance on the annual scale over land, where the solid surface interferes with microwave

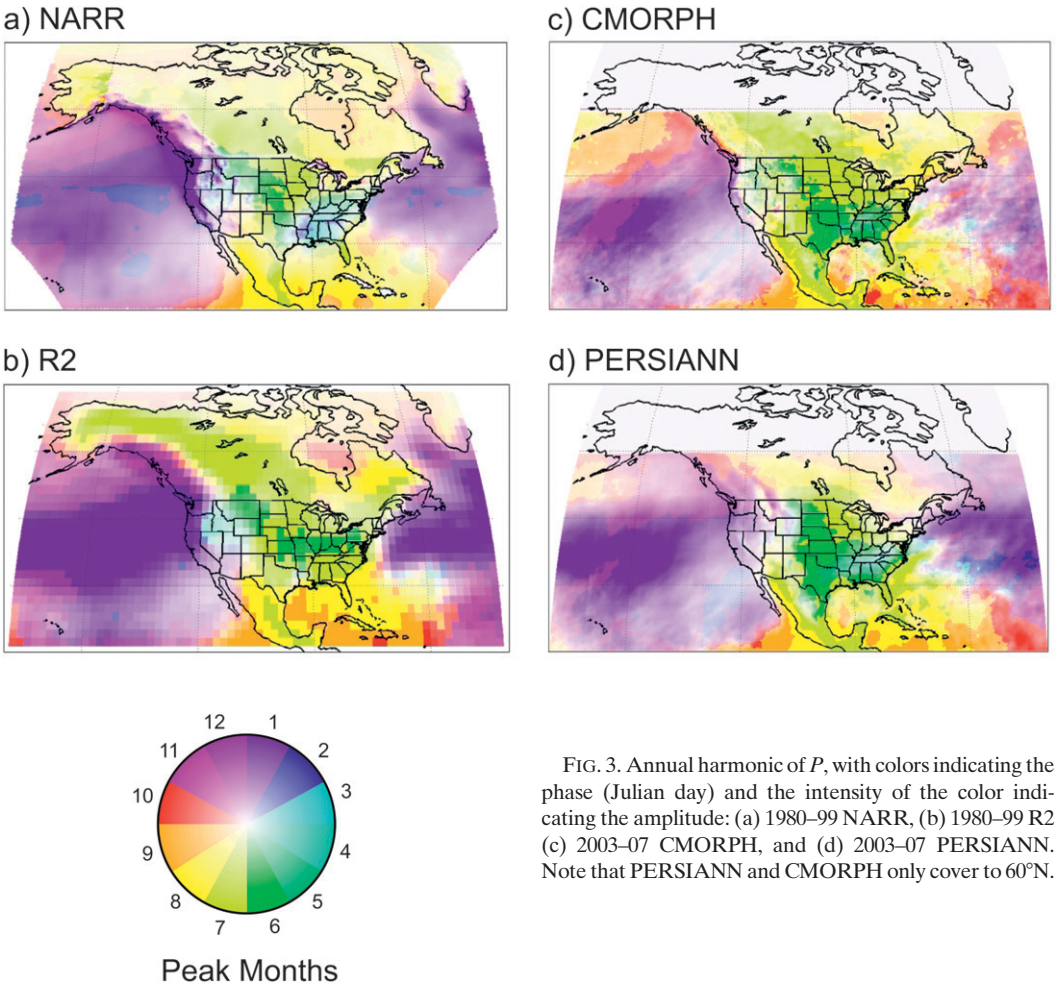

FIG. 3. Annual harmonic of P, with colors indicating the phase (Julian day) and the intensity of the color indicating the amplitude: (a) 1980–99 NARR, (b) 1980–99 R2 (c) 2003–07 CMORPH, and (d) 2003–07 PERSIANN. Note that PERSIANN and CMORPH only cover to 60°N.

retrieval algorithms for HRPP rain rates. The short record of the HRPPs constrains the utility of the comparison, however.

NARR's annual harmonic reveals several distinct annual characteristics over the North American domain. Most of the continent experiences peak rainfall in the early summertime when surface air temperatures and insolation are high, suggesting convective activity driven by locally unstable conditions. This behavior is present in all four precipitation sets, although the R2 and CMORPH have stronger annual signals with a slightly earlier phase. The lee foothills of the Rockies and the western American plains peak slightly ahead of this general continental schedule in all the precipitation sets, although the exact patterns differ slightly. The phase in these regions suggests a peak during the overlapping transition from stratiform to convective system behavior. A delay in annual phase from early to late summer, progressing from west to east across the continent, is present in all sets. Aside from the subtropical west Atlantic, which peaks in the mid-to late summer, wintertime precipitation dominates the oceans. The arrival of these wintertime storms controls annual variation over the western coasts of the United States and Canada, although the extent to which this signal penetrates into the interior mountains and dry Great Basin is greatly reduced in CMORPH. Over NARR's southeastern United States, a preference for precipitation in the late winter or early spring is identified, although the weak annual signal (particularly compared to the high mean totals) suggests that this region is sensitive to interannual variation. This signal is clear in PERSIANN and visible in CMORPH, but it absent in the R2. The HRPP also detect an early-summer precipitation maximum over the Gulf Stream that is not found by the oceanic CMAP record assimilated into NARR.

The normalized covariances that describe the annual variance of assimilated precipitation and the model precipitation estimate [Eq. (5)] through their interactions with the other water cycle components are shown in Fig. 4.

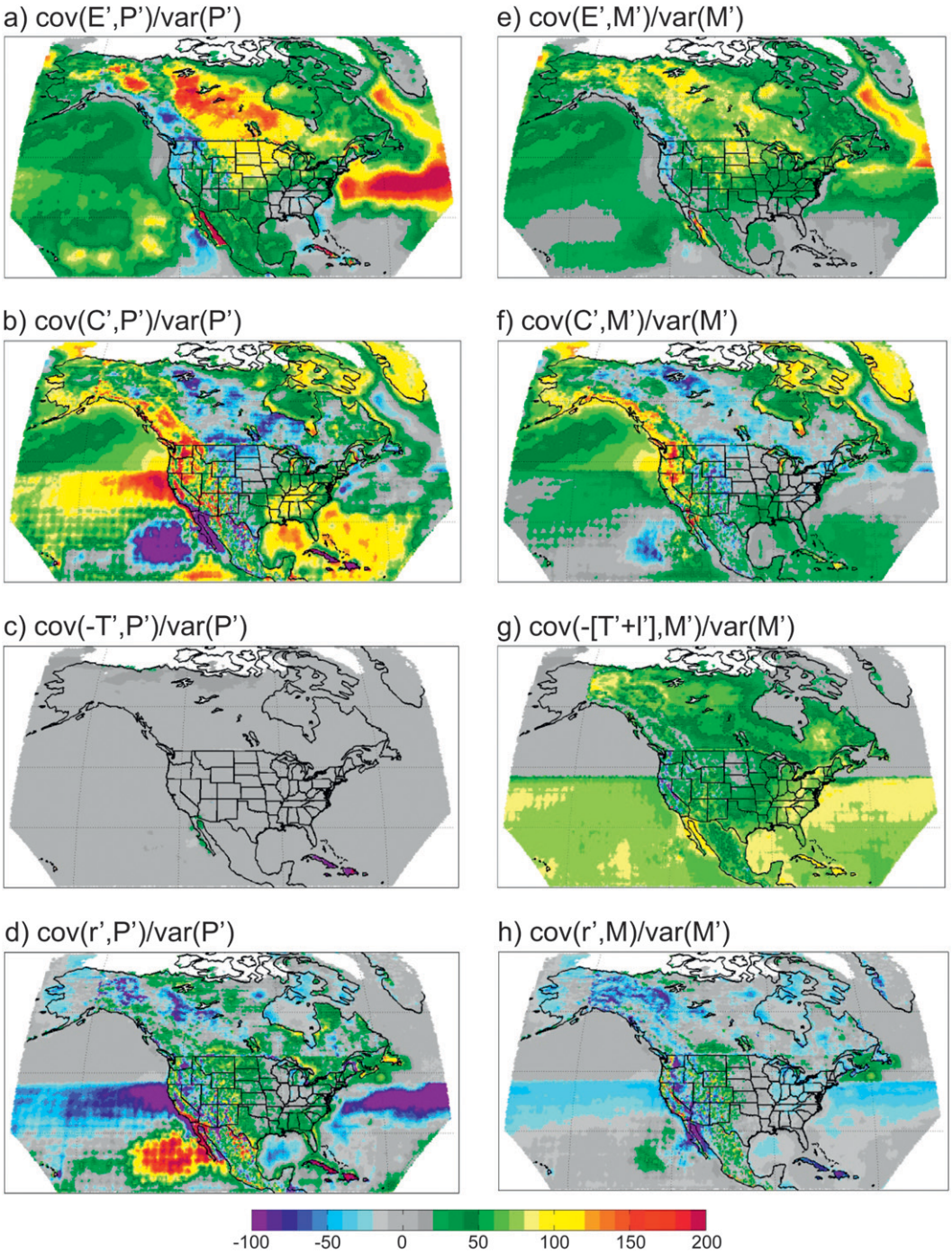

FIG. 4. The 1980–99 mean normalized covariances (%) of annual P', with each of the other water cycle components for (a)–(d) assimilated precipitation and (e)–(g) model precipitation estimate. Each row shows the normalized covariance of precipitation with (a),(e) evaporation; (b),(f) moisture flux convergence; (c),(g) negative precipitable water tendency; and (d),(h) the water budget residual for the column. The sum of the four figures in each column therefore explains 100% of the annual variance of (assimilated or model) precipitation according to Eqs. (10a) and (10b), and the areas with the lowest 5% of annual precipitation variance are omitted.

According to Eqs. (10a) and (10b), the sum of the four panels in each column is equal to 100% at every location.

Figures 4a–d describe the annual variance of the assimilated precipitation that is in the NARR output. As was suggested by the annual harmonic's phase, most of the continental interior's annual variation is dominated by an exchange between precipitation and evaporation. In large parts of Canada, the annual variance of evaporation exceeds precipitation and is balanced by a relative decrease in moisture flux convergence or a negative residual error. Over the upper Midwest and upper Great Plains of the United States, annual precipitation and evaporation vary almost identically, with annual variations of moisture flux divergence balanced out by residual error. The strong coupling between the annual variations of precipitation and evaporation decreases toward the eastern portions of the continent, where moisture flux convergence contributes moisture for precipitation and additional shortfalls are captured in the residual error term. Moisture that precipitates along the West Coast is supplied almost entirely by wintertime synoptic storms and associated moisture flux convergence, whose annual variance often exceeds precipitation. The excess moisture is balanced by an anticorrelated evaporative signal that acts as a relative source of summertime moisture as well as an imbalance captured by the residual error term. Annual precipitation variations over the southeastern United States are driven almost exclusively by annual variation of moisture flux convergence, which arrives in different seasons from year to year depending on the strength of teleconnections, as evidenced by its weak annual harmonic (Fig. 3a). Precipitable water tendency has a negligible effect on annual precipitation, as discussed in the previous section.

The percentage variance of annual precipitation described by its normalized covariance with the residual error term (Fig. 4d) is significant across wide portions of the NARR domain. The influence of the model analysis increment, both positive and negative, is clear across the mountainous portions of the continent where complex orography and mesoscale dynamics cause rapid deviations between the model and assimilated observations. In many cases these are caused (or counteracted) by deviations in the dynamical moisture flux convergence term. The annual variation of the residual error term is largely unrelated to precipitation in areas without precipitation assimilation; however, where precipitation assimilation occurs, it is an important element in the annual water cycle balance.

The normalized covariance of precipitation with the residual error term also reveals the role of precipitation assimilation increments (Figs. 2c and 2d) that interact with evaporation and moisture flux convergence extremes. The annual variation of the residual error term is particularly active in closing the annual water budget over the oceans. In the Atlantic, large, negative normalized covariances of precipitation with residual error match a region of high precipitation assimilation and balance an excess in annual evaporation. In the eastern Pacific, strong moisture flux convergence relationships with precipitation (Fig. 4b) are offset by the residual error term. Wintertime storms that are prevalent off the coast of California sweep down from the North Pacific, where precipitation assimilation is absent, leading to seasonally varying airmass adjustments south of 42.5°N that come largely from the error term. Scant rainfall in the stratocumulus regions off the coast of Mexico and in the Sea of Cortez comes in a season with relatively high moisture flux divergence, a process that evidently is not captured in NARR's underlying model but is value added by the assimilation process.

Figures 4e–h describe the annual variation of the model precipitation estimate. The basic continental features of variation explained by covariation with evaporation (Fig. 4e) are similar to the features explaining the assimilated precipitation recorded in the NARR output (Fig. 4a), although the magnitudes of extremes (away from 100%) are reduced. Therefore, evaporation's annual variations are more in line with the higher model precipitation estimate than with the assimilated precipitation.

Interactions between moisture flux convergence and the model precipitation estimate at the annual time scale also have reduced extremes, but entirely new geographical patterns emerge. Over the southeastern United States and the subtropical Atlantic, moisture flux convergence shows very little interaction with the model precipitation estimate (Fig. 4f), but it explains nearly 100% of the assimilated precipitation reported in NARR (Fig. 4b). In these regions precipitation assimilation reveals a seasonal water cycle exchange between these two components that was not captured in the underlying model. The strong normalized covariances of precipitation and moisture flux convergence in the southeastern United States, along with high mean rainfall (Fig. 1a) and low amplitude in the seasonal harmonic (Fig. 3a), are the signature of a region strongly affected by teleconnections, which govern peak rainfall independent of the consistent annual cycle of direct solar forcing.

Declines in the amount of model precipitation estimate variance described by evaporation and moisture flux convergence are offset by large percentages of variance described by the negative sum of precipitable water tendency and the precipitation assimilation increments (Fig. 4g). Moisture contributed through these terms is highest over the oceans, the Yukon Territory, Quebec,

and the eastern United States. In these areas, the annual variation of precipitation in NARR output is especially dependent on contributions from the precipitation assimilation scheme.

In general, normalized covariance of the model precipitation estimate with the residual error term (Fig. 4h) is much smaller in magnitude than the corresponding normalized covariance of assimilated precipitation (Fig. 4d). One consequence of the model precipitation estimate [recall Eqs. (5) and (6)] is that the precipitation assimilation increment (I') is largely cancelled out of the normalized covariance of M' and r'. Figure 4h, therefore, estimates the residual error relationship before precipitation assimilation occurs, dominated by features over the complex terrain of the western mountains that are likely caused by the model analysis increment. Because the estimation of M' cannot capture the discrepancy between 3-hourly output and the hourly precipitation assimilation, some aspects of precipitation assimilation persist even in Fig. 4h—for example, over the fast-moving synoptic storms in the oceanic band wherein CMAP precipitation is blended. Precipitation assimilation allows for a more realistic representation of precipitation variability; however, to force these corrections, the precipitation assimilation scheme produces larger annual water cycle imbalances in the theoretical water balance over most of NARR's domain. For any region of interest, however, analysis of Fig. 4 provides the sign and geographical pattern of these imbalances and their associated component biases, benefitting the interpretation of applications and impact studies driven by NARR output and potentially prioritizing areas for improvement in future reanalyses.

According to Eq. (1), annual variance of precipitation would be explained entirely by its normalized covariances with evaporation and moisture flux convergence, as annual precipitable water tendencies are negligible. Figure 5 shows the extent to which these natural components explain both assimilated precipitation and the model precipitation estimate. Over the northern oceans (where there is no precipitation assimilation), these terms describe 100% of precipitation's variance, although small areas have an apparent residual term likely due to the model analysis increment. Compared to the model precipitation estimate, the assimilated precipitation is described more completely by the natural components over nearly the entire domain. In many areas, however, NARR precipitation is overdescribed (normalized covariance of precipitation with evaporation and moisture flux convergence is greater than 100%), leading to excessive moisture imbalances. In these areas NARR's underlying model produced high precipitation rates that were reduced by precipitation assimilation; however, the other components

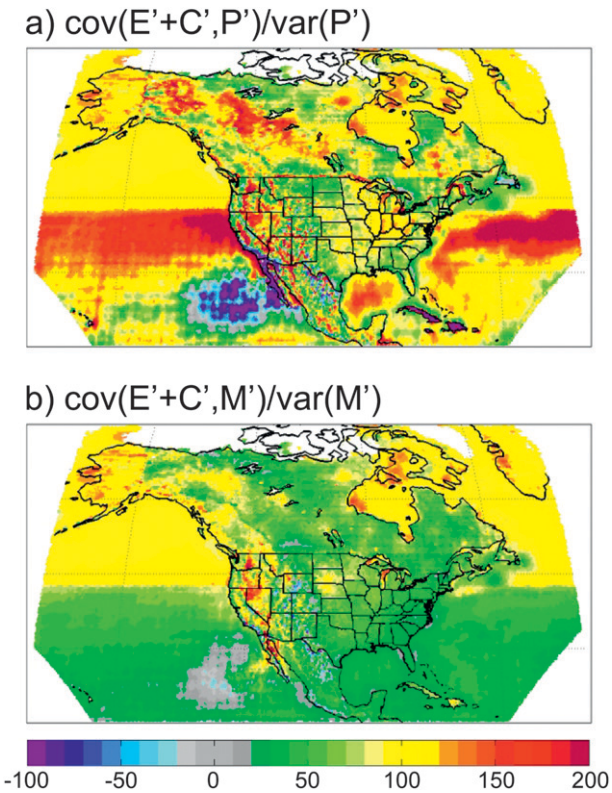

FIG. 5. The 1980–99 mean normalized covariances (%) of annual (a) assimilated precipitation and (b) the model precipitation estimate with the sum of evaporation and convergence variations.

in this (too vigorous) water cycle were not likewise reduced. As discussed earlier, this overly strong annual evaporation in NARR has been hypothesized (Nigam and Ruiz-Barradas 2006; Kanamaru and Kanamitsu 2007), but it is more clearly demonstrated here by comparing the water cycle balances before and after precipitation assimilation.

To further elucidate the effect of precipitation assimilation on annual precipitation, Fig. 6 shows the normalized covariance of the assimilated precipitation with its model and assimilation increment terms. According to Eqs. (3) and (5), the sum of the three panels explains 100% of the assimilated precipitation's annual variance at every location. The model and assimilated precipitation are equivalent in the areas without precipitation assimilation as well as approximately equivalent across a broad swath of the Great Plains states, the Great Basin, the Canadian Rockies, and the stratocumulus precipitation minimum west of Baja California. Across most of the areas where precipitation assimilation occurs, the model precipitation's annual variation is in phase with assimilated precipitation but with much larger amplitude, reflecting the overactive hydrologic cycle in the underlying model.

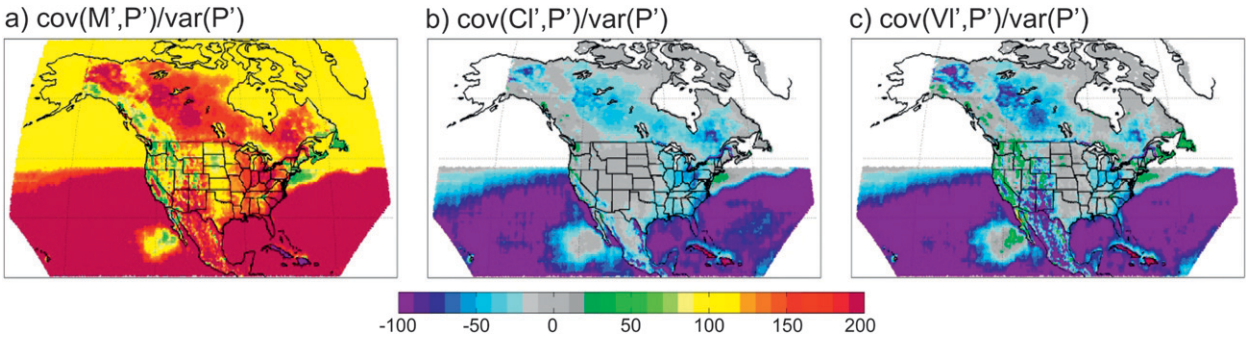

FIG. 6. The 1980–99 mean normalized covariances (%) of annual assimilated precipitation with each of its assimilation components: (a) model precipitation estimate, (b) condensate increment, and (c) vapor increment. The sum of the three panels therefore explains 100% of the assimilated P' according to Eqs. (3) and (5). Note that the white areas in (b) and (c) did not undergo precipitation assimilation.

Excess model precipitation variance on the annual time scale is matched mostly by reductions from the assimilation increment terms (Figs. 6b and 6c). Over the oceans both the vapor and condensate increment make large adjustments, with the vapor increment term slightly larger in magnitude. The vapor increment also has a larger influence over central and western Canada, while the condensate increment is more substantial over the eastern portions of the United States and Canada (indicating an excess in cloud mass). Precipitation assimilation over the mountainous portions of the western United States and Mexico is dominated by the vapor increment on the annual time scale. Over the arid southwestern United States and Mexico, annual assimilated precipitation is associated with large reductions in column water vapor, suggesting that the lower atmosphere is too moist in the underlying Eta model. Over the northern portions of the U.S. Rockies, the Pacific Northwest, and California, the annual variation of M' is less than or shifted in phase from P'. In these areas, which have significant annual variation in C', the seasonal cycle of precipitation is enhanced locally by precipitation assimilation corrections made largely through the vapor increment term.

6. Summary, discussion, and future work

The NCEP North American Regional Reanalysis is appealing for use in continuing applications and climate impact assessments, as it provides one of the best climatological datasets over North America, with high-spatial-and-temporal-resolution water budget components constrained by precipitation assimilation and archived over a 20-plus-yr period. In light of the high potential for the use of NARR output, this study examined the 20-yr mean hydroclimatology (seen in NARR at higher detail than in any other large-scale reanalysis) and identified regional annual component interactions in the atmospheric water cycle using a normalized covariance metric that describes the variance in precipitation as explained by its covariance with the other water cycle components. Mean summertime conditions and diurnal variations are examined using similar metrics in Part II of this study, examining NARR's improvement of water cycle interactions around convective activity.

This climatology of annual moisture exchange is critical to understanding the processes governing local climates across the continent, as well as how they may change in a future climate, and is a new way of examining a transient water cycle balance. Areas where seasonal precipitation draws largely from evaporation are sensitive to processes affecting atmospheric stability, including land surface interactions, boundary layer physics, and convective processes. Regions where seasonal precipitation draws largely from moisture flux convergence are sensitive to dynamical processes, either large-scale waves and circulations or conditions that favor the development and propagation of mesoscale activity.

Initial analyses noted biases caused when NARR's precipitation assimilation scheme reduced precipitation from an overactive hydrological cycle in the underlying model, which was characterized using an estimate of the underlying model precipitation to assist in the interpretation of bias and uncertainty in NARR applications and water budget studies. These estimates show that precipitation assimilation is overwhelmingly used to reduce overactive model precipitation, particularly over the oceans and the eastern part of the continent. Other components of the water cycle are not similarly reduced during the assimilation process, resulting in biases where evaporation and moisture flux convergence are tied to a more vigorous water cycle than is the corrected precipitation. NARR remains a recommended candidate for use in applications and impact assessment studies, as the benefits of precipitation assimilation are clear and the side effects may be characterized. The analyses

presented here depict these biases spatially and temporally to allow NARR users to more accurately interpret results, to identify areas that may be improved in future reanalyses, and to identify areas where the budget is currently closed with minimal residual error.

The maps presented here have too many features to comprehensively analyze in this space, but future work may continue to shed light on the characteristic regional patterns that emerge and their sensitivities to observational datasets, reanalysis systems, climate models, and future climate scenarios. For example, the signature of teleconnections, identified over the southeastern United States, could be sought in other regions and under future scenarios. NARR provides a good benchmark for comparing high-resolution precipitation product algorithms on this long time scale in regions of precipitation assimilation, revealing challenges in capturing the inland extent of wintertime storms as well as interannual variability over the southeastern United States. Additionally, these results form a basis for an intercomparison of precipitation assimilation schemes, other reanalysis products, or climate models that could use these metrics to put NARR's performance in the context of other available products. Lastly, conducting these analyses on climate change scenarios would characterize the projected sensitivity of component interactions to climate changes, with large societal implications tied to potential regime shifts.

Acknowledgments. This research was supported by an appointment to the NASA Postdoctoral Program at the Goddard Institute for Space Studies, administered by Oak Ridge Associated Universities (ORAU) through a contract with NASA. The views expressed herein are those of the author and do not necessarily reflect the views of NASA or ORAU. The author would like to thank Ernesto Hugo Berbery and Fedor Mesinger for their early discussions about NARR's water cycle, Ying Lin for her extensive assistance in revisiting NARR's precipitation assimilation scheme, Radley Horton for his multiple edits, Masao Kanamitsu for his helpful advice, and three anonymous reviewers for their helpful comments.

REFERENCES

Anderson, B. T., A. C. Ruane, J. O. Roads, and M. Kanamitsu, 2009: Estimating the influence of evaporation and moisture-flux convergence upon seasonal precipitation rates. Part II: An analysis for North America based upon the NCEP–DOE Reanalysis II model. *J. Hydrometeor.,* **10,** 893–911.

Becker, E. J., and E. H. Berbery, 2008: The diurnal cycle of precipitation over the North American monsoon region during the NAME 2004 field campaign. *J. Climate,* **21,** 771–787.

Berbery, E. H., E. M. Rasmusson, and K. E. Mitchell, 1996: Studies of North American continental-scale hydrology using Eta model forecast products. *J. Geophys. Res.,* **101** (D3), 7305–7319.

Betts, A. K., J. H. Ball, and P. Viterbo, 1999: Basin-scale surface water and energy budgets for the Mississippi from the ECMWF reanalysis. *J. Geophys. Res.,* **104** (D16), 19 293–19 306.

Black, T. L., 1994: The new NMC mesoscale eta model: Description and forecast samples. *Wea. Forecasting,* **9,** 265–278.

Bukovsky, M. S., and D. J. Karoly, 2007: A brief evaluation of precipitation from the North American Regional Reanalysis. *J. Hydrometeor.,* **8,** 837–846.

Daly, C., R. P. Neilson, and D. L. Phillips, 1994: A statistical–topographic model for mapping climatological precipitation over mountainous terrain. *J. Appl. Meteor.,* **33,** 140–158.

Dirmeyer, P. A., and K. L. Brubaker, 2007: Characterization of the global hydrologic cycle from a back-trajectory analysis of atmospheric water vapor. *J. Hydrometeor.,* **8,** 20–37.

Dominguez, F., and P. Kumar, 2008: Precipitation recycling variability and ecoclimatological stability—A study using NARR data. Part I: Central U.S. plains ecoregion. *J. Climate,* **21,** 5165–5186.

Ek, M. B., K. E. Mitchell, Y. Lin, E. Rogers, P. Grunmann, V. Koren, G. Gayno, and J. D. Tarpley, 2003: Implementation of Noah land surface model advances in the National Centers for Environmental Prediction operational mesoscale Eta model. *J. Geophys. Res.,* **108,** 8851, doi:10.1029/2002JD003296.

Higgins, R. W., Y. Yao, E. S. Yarosh, J. E. Janowiak, and K. C. Mo, 1997: Influence of the Great Plains low-level jet on summertime precipitation and moisture transport over the central United States. *J. Climate,* **10,** 481–507.

——, W. Shi, E. Yarosh, and R. Joyce, 2000: *Improved United States Precipitation Quality Control System and Analysis*. NCEP/Climate Prediction Center Atlas 7, NOAA/NWS, 40 pp.

——, and Coauthors, 2006: The NAME 2004 field campaign and modeling strategy. *Bull. Amer. Meteor. Soc.,* **87,** 79–94.

Hsu, K., X. Gao, S. Sorooshian, and H. V. Gupta, 1997: Precipitation estimation from remotely sensed information using artificial neural networks. *J. Appl. Meteor.,* **36,** 1176–1190.

Janjić, Z. I., 1994: The step-mountain eta coordinate model: Further developments of the convection, viscous sublayer, and turbulence closure schemes. *Mon. Wea. Rev.,* **122,** 927–945.

——, 1997: Advection scheme for passive substances in the NCEP Eta model. *Research Activities in Atmospheric and Oceanic Modelling,* WMO, 3.14.

Joyce, R. J., J. E. Janowiak, P. A. Arkin, and P. Xie, 2004: CMORPH: A method that produces global precipitation estimates from passive microwave and infrared data at high spatial and temporal resolution. *J. Hydrometeor.,* **5,** 487–503.

Kanamaru, H., and M. Kanamitsu, 2007: Fifty-seven-year California Reanalysis Downscaling at 10 km (CaRD10). Part II: Comparison with North American Regional Reanalysis. *J. Climate,* **20,** 5572–5592.

Kanamitsu, M., W. Ebisuzaki, J. Woollen, S.-K. Yang, J. Hnilo, M. Fiorino, and J. Potter, 2002: NCEP–DOE AMIP-II reanalysis (R-2). *Bull. Amer. Meteor. Soc.,* **83,** 1631–1643.

Karnauskas, K. B., A. Ruiz-Barradas, S. Nigam, and A. J. Busalacchi, 2008: North American droughts in ERA-40 global and NCEP North American regional reanalyses: A Palmer drought severity index perspective. *J. Climate,* **21,** 2102–2123.

Krishnamurti, T. N., K. Ingles, S. Cocke, R. Pasch, and T. Kitade, 1984: Details of low latitude medium range numerical weather prediction using a global spectral model. Part II: Effect of orography and physical initialization. *J. Meteor. Soc. Japan.,* **62,** 613–649.

Lin, Y., K. E. Mitchell, M. E. Baldwin, E. Rogers, and G. DiMego, 1999: Test assimilations of the real-time, multi-sensor hourly precipitation analysis into the NCEP Eta Model. Preprints, *Eighth Conf. on Mesoscale Processes,* Boulder, CO, Amer. Meteor. Soc., 341–344. [Available online at http://www.emc.ncep.noaa.gov/mmb/papers/lin/pcpasm/paper.html.]

Luo, Y., E. H. Berbery, K. E. Mitchell, and A. Betts, 2007: Relationships between land surface and near-surface atmospheric variables in the NCEP North American Regional Reanalysis. *J. Hydrometeor.,* **8,** 1184–1203.

Mearns, L. O., W. Gutowski, R. Jones, R. Leung, S. McGinnis, A. Nunes, and Y. Qian, 2009: A regional climate change assessment program for North America. *Eos, Trans. Amer. Geophys. Union,* **90,** doi:10.1029/2009EO360002.

Mesinger, F., and Coauthors, 2006: North American Regional Reanalysis. *Bull. Amer. Meteor. Soc.,* **87,** 343–360.

Mo, K. C., M. Chelliah, M. L. Carrera, R. W. Higgins, and W. Ebisuzaki, 2005: Atmospheric moisture transport over the United States and Mexico as evaluated in the NCEP regional reanalysis. *J. Hydrometeor.,* **6,** 710–728.

Monobianco, J., S. Koch, V. M. Karyampudi, and A. J. Negri, 1994: The impact of assimilating satellite-derived precipitation rates on numerical simulations of the ERICA IOP 4 cyclone. *Mon. Wea. Rev.,* **122,** 341–365.

Nigam, S., and A. Ruiz-Barradas, 2006: Seasonal hydroclimate variability over North America in global and regional reanalyses and AMIP simulations: Varied representation. *J. Climate,* **19,** 815–837.

Nunes, A. M. B., and J. O. Roads, 2005: Improving regional model simulations with precipitation assimilation. *Earth Interactions,* **9.** [Available online at http://EarthInteractions.org.]

——, and ——, 2007: Influence of precipitation assimilation on a regional climate model's surface water and energy budgets. *J. Hydrometeor.,* **8,** 642–664.

Rasmusson, E. M., 1967: Atmospheric water vapor transport and the water balance of North America: Part I. Characteristics of the water vapor flux field. *Mon. Wea. Rev.,* **95,** 403–426.

——, 1968: Atmospheric water vapor transport and the water balance of North America: Part II. Large-scale water balance investigations. *Mon. Wea. Rev.,* **96,** 720–734.

Roads, J. O., M. Kanamitsu, and R. Stewart, 2002: CSE water and energy budgets in the NCEP–DOE Reanalysis II. *J. Hydrometeor.,* **3,** 227–248.

——, and Coauthors, 2003: GCIP water and energy budget synthesis (WEBS). *J. Geophys. Res.,* **108,** 8609, doi:10.1029/2002JD002583.

Rogers, E., M. Ek, Y. Lin, K. Mitchell, D. Parrish, and G. DiMego, 2001: Changes to the NCEP Meso Eta analysis and forecast system: Assimilation of observed precipitation, upgrades to land-surface physics, modified 3DVAR analysis. NWS Tech. Procedures Bull. 473, 10 pp.

Ruane, A. C., 2010: NARR's atmospheric water cycle components. Part II: Summertime mean and diurnal interactions. *J. Hydrometeor.,* **11,** 1220–1233.

——, and J. O. Roads, 2007a: 6-hour to 1-year variance of five global precipitation sets. *Earth Interactions,* **11.** [Available online at http://EarthInteractions.org.]

——, and ——, 2007b: The diurnal cycle of water and energy over the continental United States from three reanalyses. *J. Meteor. Soc. Japan,* **85A,** 117–143.

——, and ——, 2008: Dominant balances and exchanges of the atmospheric water cycle in the Reanalysis 2 at diurnal, annual, and intraseasonal time scales. *J. Climate,* **21,** 3951–3966.

Ruiz-Barradas, A., and S. Nigam, 2006: Great Plains hydroclimate variability: The view from North American Regional Reanalysis. *J. Climate,* **19,** 3004–3010.

Schubert, S., and Y. Chang, 1996: An objective method for inferring sources of model error. *Mon. Wea. Rev.,* **124,** 325–340.

Shafran, P. C., J. Woollen, W. Ebisuzaki, W. Shi, Y. Fan, R. W. Grumbine, and M. Fennessy, 2004: Observational data used for assimilation in the NCEP North American Regional Reanalysis. Preprints, *14th Conf. on Applied Climatology,* Seattle, WA, Amer. Meteor. Soc., 1.4. [Available online at http://ams.confex.com/ams/84Annual/techprogram/paper_71689.htm.]

Solomon, S., D. Qin, M. Manning, M. Marquis, K. Averyt, M. M. B. Tignor, H. L. Miller Jr., and Z. Chen, Eds., 2007: *Climate Change 2007: The Physical Sciences Basis*. Cambridge University Press, 996 pp.

Szeto, K. K., H. Tran, M. D. MacKay, R. Crawford, and R. E. Stewart, 2008: The MAGS water and energy budget study. *J. Hydrometeor.,* **9,** 96–115.

Trenberth, K. E., and C. J. Guillemot, 1998: Evaluation of the atmospheric moisture and hydrologic cycle in the NCEP/NCAR reanalyses. *Climate Dyn.,* **14,** 213–231.

——, A. Dai, R. M. Rasmussen, and D. B. Parsons, 2003: The changing character of precipitation. *Bull. Amer. Meteor. Soc.,* **84,** 1205–1217.

Vivoni, E. R., H. Moreno, G. Mascaro, J. C. Rodriguez, C. J. Watts, J. Garatuza-Payan, and R. L. Scott, 2008: Observed relation between evapotranspiration and soil moisture in the North American monsoon region. *Geophys. Res. Lett.,* **35,** L22403, doi:10.1029/2008GL036001.

West, G. L., W. J. Steenburgh, and W. Y. Y. Cheng, 2007: Spurious grid-scale precipitation in the North American Regional Reanalysis. *Mon. Wea. Rev.,* **135,** 2168–2184.

Xie, P., and P. A. Arkin, 1997: Global precipitation: A 17-year monthly analysis based on gauge observations, satellite estimates, and numerical model outputs. *Bull. Amer. Meteor. Soc.,* **78,** 2539–2558.

Yap, K.-S., 1995: Impact of Newtonian assimilation and physical initialization on the initialization and prediction by a tropical mesoscale model. *Mon. Wea. Rev.,* **123,** 833–861.

Yilmaz, K. K., H. V. Gupta, and T. Wagener, 2008: A process-based diagnostic approach to model evaluation: Application to the NWS distributed hydrologic model. *Water Resour. Res.,* **44,** W09417, doi:10.1029/2007WR006716.